Low Earth orbit satellite navigation errors and vertical total electron content in single-frequency GPS tracking

Miquel Garcia-Fernàndez[1] and Oliver Montenbruck[1]

[1]   In the context of space applications, the GPS system is presently a well-established and accepted tracking system. To meet the basic navigation requirements, most satellites in a low Earth orbit are equipped with single-frequency GPS receivers that measure the coarse acquisition code as well as the L1 phase. However, the resulting kinematic navigation solutions exhibit systematic position errors caused by elevation-dependent ionospheric path delays. In this study a simple analytical model is established, which quantitatively relates the position error to the vertical electron content and the mapping function. This model substantiates the empirical evidence of a mean radial offset that increases in proportion to the total electron content above the satellite. It is furthermore shown that the ratio between this offset and the vertical ionospheric path delay depends on the applied elevation mask angle. Representative ratios of 3–5 are obtained for the mapping function of the Lear ionosphere model and elevation cutoff angles of 10°, 5°, and 0°. This analytical result has further been confirmed by signal simulator tests as well as flight data of the CHAMP satellite.

1.   Introduction

[2] Since the firsts efforts on using the GPS system for space applications [see, e.g., *Yunck et al.*, 1994], GPS receivers have evolved into a mature and widely used tracking system for satellites in a low Earth orbit (LEO). However, since the basic positioning requirements for space applications are well met with single-frequency GPS data, the vast majority of GPS system onboard a LEO rely only on coarse acquisition (C/A) code and L1 phase measurements.

[3] As it is known, the ionosphere is the most important error source when working with single-frequency GPS receivers. While dual-frequency GPS receivers can take advantage of the dispersive nature of the ionosphere and remove its effect with a suitable combination of observables, single-frequency receivers have to rely on external models such as the Klobuchar model [*Klobuchar*, 1996] or the global ionospheric maps (GIM) of vertical total electron content [see, e.g., *Feltens and Schaer*, 1998]. As

---

[1]German Space Operation Center, Deutsches Zentrum fur Luft- und Raumfahrt, Wessling, Germany.

an example, meter level orbit determination of LEO satellites using GIMs has been demonstrated by *Montenbruck and Gill* [2002] and *Hwang and Born* [2005]. As an alternative to model-based corrections, a rigorous elimination of ionospheric errors can be achieved through the Group and Phase Ionospheric Correction (GRAPHIC) [*Yunck*, 1996] combination of single-frequency code carrier measurements. Recent works that have successfully applied this technique for dynamic and kinematic orbit determination include *Berthias et al.* [2001], *Yoon et al.* [2002], and *Montenbruck* [2003].

[4] For kinematic real-time navigation of LEO satellites neither of the aforementioned methods is applicable and manufacturers of spaceborne GPS receivers have commonly preferred to leave the position solution uncorrected from ionospheric effects. This can be justified for high-altitude orbits (>1000 km) with a very low vertical total electron content (VTEC) above the spacecraft. However, it may introduce position errors of several tens of meters for orbital altitudes close to the ionospheric electron density maximum (300–400 km). As pointed out by *Berthias et al.* [2001] and *Montenbruck and Gill* [2002], the resulting navigation errors exhibit a systematic radial bias, which has been attributed to the elevation dependence of the ionospheric path delays.

[5] Within this paper an analytical model for the radial position offset in uncorrected single-frequency navigation solutions is established. It provides a simple relation between position errors, vertical TEC and the applied elevation mask, which can be used to assess the expected navigation accuracy in a premission analysis. Vice versa this relation may be used to infer approximate VTEC values above the spacecraft if the radial bias can be independently determined from a dynamic orbit adjustment. Compared to other methods for ionospheric parameter retrieval from single-frequency GPS measurements [*Van Dierendonck et al.*, 1993; *Montenbruck and Markgraf*, 2003], this approach does not require raw code and carrier phase data. Given the fact that most satellites provide only GPS navigation solutions but no raw measurements for ground operations, the present method is thus applicable to a much wider range of missions. This might open a way for monitoring the state of the ionosphere with adequate temporal and regional resolution using single-frequency navigation solutions from a large set of orbiting spacecraft.

2. Kinematic Positioning and Ionospheric Path Delays

[6] As it is well known, the single point position solution in a GPS receiver is obtained through a least squares adjustment of the vector

$$\mathbf{x} = (x, y, z, c\delta t) \tag{1}$$

formed by the position components (x, y and z) and the clock offset ($c\delta t$) with the criterion of minimizing the RMS difference between the n observed and modeled pseudoranges [see, e.g., *Misra and Enge*, 2001]. Considering the vector $\mathbf{I}$ with the unmodeled ionospheric delays for the n observed GPS satellites, the error of the navigation solution can be expressed as

$$\Delta\mathbf{x} = \left(\mathbf{G}^T\mathbf{G}\right)^{-1}\mathbf{G}^T\mathbf{I}. \tag{2}$$

Here $\mathbf{G}$ is the design matrix containing the line-of-sight unit vectors from the receiving antenna to the transmitting satellite. Adopting a local horizontal east-north-up reference system and employing the polar angles azimuth (A) and elevation (E) to describe the viewing directions, the $\mathbf{G}$ matrix can be written as

$$\mathbf{G} = \begin{pmatrix} -\sin A_1 \cos E_1 & -\cos A_1 \cos E_1 & -\sin E_1 & +1 \\ \vdots & \vdots & \vdots & \vdots \\ -\sin A_n \cos E_n & -\cos A_n \cos E_n & -\sin E_n & +1 \end{pmatrix}. \tag{3}$$

Using equations (1) to (3), the impact of the ionospheric errors on the navigation solution can be evaluated for a particular set of observed GPS satellites and the ionospheric path delays. However, it would be interesting to have a more general analysis and provide a statistical theoretical assessment of the resulting position errors. To do this, let us assume that the observable GPS satellites are, on average, evenly distributed on the celestial sphere. Assuming a total of n satellites in a hemisphere and an elevation mask of E_0, one can express the probability of observing a satellite in a surface element da over a hemisphere delimited by the elevation mask as

$$p(a)da = \frac{n \, da}{2\pi(1 - \sin(E_0))}. \tag{4}$$

In evaluating the $\mathbf{G}^T\mathbf{G}$ and $\mathbf{G}^T\mathbf{I}$ products, the expectation of the sums

$$\sum_{i=1}^{n} (*) \tag{5}$$

over all observed satellites may thus be replaced by integrals

$$\oint_{E>E_0} (*)p(a)da =$$

$$\frac{n}{2\pi(1 - \sin E_0)} \int_{E_0}^{\pi/2} \int_{0}^{2\pi} (*) \cos E \, dA \, dE \tag{6}$$

over the visible part of the celestial sphere. The particular structure of the design matrix allows the factorization of all double integrals into azimuth and elevation-dependent terms. After performing the azimuth integral over angles between 0 and 2π, numerous terms vanish, leaving only two off-diagonal terms with nonzero value. After substituting the sums and arranging the products, the resulting normal equations matrix can be expressed as

$$\mathbf{G}^T\mathbf{G} = \frac{n}{1-\sin E_0} \begin{pmatrix} N_{11} & 0 & 0 & 0 \\ 0 & N_{22} & 0 & 0 \\ 0 & 0 & N_{33} & N_{34} \\ 0 & 0 & N_{43} & N_{44} \end{pmatrix}, \tag{7}$$

where the only nontrivial elements are given by

$$N_{11} = N_{22} = \frac{1}{3} - \frac{1}{2}\sin E_0 + \frac{1}{6}\sin^3 E_0$$

$$N_{33} = \frac{1}{3} - \frac{1}{3}\sin^3 E_0 \tag{8}$$

$$N_{34} = N_{43} = -\frac{1}{2} + \frac{1}{2}\sin^2 E_0$$

$$N_{44} = 1 - \sin E_0.$$

Table 1. Average Vertical Position Error (Δr) and Clock Offset Error $\Delta c\delta t$ Due to Unconsidered Ionospheric Path Delays at the L1 Frequency, Assuming a Lear Mapping Function and Elevation Thresholds of $E_0 = 0°$, $5°$, and $10°$

E_0	$0°$, m/TECU	$5°$, m/TECU	$10°$, m/TECU
Δr/VTEC	0.81	0.64	0.52
$\Delta c\delta t$/VTEC	0.82	0.70	0.61

The block diagonal structure of the normal equation matrix allows for a simple analytical inversion yielding the resulting expression

$$\left(\mathbf{G}^T\mathbf{G}\right)^{-1} = \frac{1 - \sin E_0}{n} \begin{pmatrix} N_{11}^{-1} & 0 & 0 & 0 \\ 0 & N_{22}^{-1} & 0 & 0 \\ 0 & 0 & \dfrac{N_{44}}{D} & -\dfrac{N_{34}}{D} \\ 0 & 0 & -\dfrac{N_{43}}{D} & \dfrac{N_{33}}{D} \end{pmatrix} \tag{9}$$

with

$$D = N_{33}N_{44} - N_{34}N_{43}. \tag{10}$$

On the other hand, the $\mathbf{G}^T\mathbf{I}$ product can be evaluated using the same approach of integrals to obtain a statistical assessment. As it is known, the ionospheric delay

$$I = \frac{40.3}{f_{L1}^2}\frac{\text{m}^3}{\text{s}^2} \cdot \text{STEC} = 0.162\,\text{m}\frac{\text{STEC}}{\text{TECU}} \tag{11}$$

that affects the L1 C/A code pseudorange is directly proportional to the slant total electron content (STEC) along the line of sight from the GPS satellite to the receiver. Here f_{L1} designates the L1 carrier frequency (1.575 GHz) and the TEC unit is defined as 1 TECU = $10^{16} e^-/\text{m}^2$.

[7] Using a mapping function with elevation dependency $m(E)$, it is possible to convert from slant TEC to vertical TEC, leading to the following expression:

$$I(E) = 0.162\,\text{m} \cdot m(E) \cdot \frac{\text{VTEC}}{\text{TECU}}. \tag{12}$$

[8] Therefore the product $\mathbf{G}^T\mathbf{I}$ evaluates to

$$\mathbf{G}^T\mathbf{I} = \frac{n \cdot 0.162\,\text{m}}{1 - \sin E_0} \cdot \frac{\text{VTEC}}{\text{TECU}} \cdot \begin{pmatrix} 0 \\ 0 \\ b_3 \\ b_4 \end{pmatrix} \tag{13}$$

with

$$b_3 = -\int_{E_0}^{\pi/2} m(E)\sin E \cos E\, dE$$
$$b_4 = +\int_{E_0}^{\pi/2} m(E) \cos E\, dE. \tag{14}$$

For the present study we adopted the mapping function

$$m(E) = \frac{2.037}{\sqrt{\sin^2 E + 0.076} + \sin E} \tag{15}$$

that has been recommended by *Lear* [1987] for use with orbiting spacecraft. We independently verified this mapping function to closely match the results of a rigorous ray tracing for a LEO satellite at 450 km altitude using a Chapman profile [*Davies*, 1990] with scale height $H = 75$ km and a height of maximum electron density $h_mF_2 = 300$ km.

[9] After evaluation of the integrals in equation (14) and multiplication with the inverse normal equation matrix (9), numerical relations describing the position error and the clock error as a function of the VTEC above the LEO satellite are obtained. Note that the term n vanishes and therefore the obtained relations are basically independent of the number of satellites. As may be recognized from the structure of the normal equations, the horizontal components of the position vector are not affected by the neglect of ionospheric path delays in the single point navigation solution. The vertical position error (Δr) and the clock error ($\Delta c\delta t$), on the other hand, depend on the mapping function and the applied elevation mask. For a representative elevation masks of $0°$, $5°$ and $10°$, the resulting values are given in Table 1. It is recognized that the employed elevation mask has a notable impact on the resulting position and clock errors, with smaller errors obtained at higher elevation masks. Compared to a full hemispherical coverage, the errors decrease by roughly one third when constraining the observations to elevations above $10°$.

3. Data Analysis

[10] Supplementary to the analytical derivation, navigation solutions obtained with actual GPS receivers have been analyzed in order to study the occurrence of a radial position offset in single-frequency GPS tracking of LEO satellites. Appropriate test data for this assessment have been collected both in a signal simulator test bed and from current space missions. In all cases, navigation solutions are based on single-frequency measurements and do not employ any ionospheric corrections. Other than for terrestrial GPS receivers, use of the Klobuchar

Table 2. Single-Point Position Errors as Obtained in the Signal Simulator Test Bed for a 10 TECU Ionosphere Using Different Elevation Thresholds[a]

E_0	0°, m	5°, m	10°, m
ε_R	7.08 ± 2.11	6.23 ± 1.56	5.23 ± 1.23
ε_T	0.02 ± 0.80	0.00 ± 0.62	−0.02 ± 0.46
ε_N	−0.04 ± 0.76	−0.02 ± 0.55	−0.01 ± 0.43

[a]Mean values and standard deviations for a 15 hour data arc are given for the radial (R), along-track (T), and cross-track (N) components.

model makes no sense for a spaceborne vehicle. Therefore, with few exceptions, a ionospheric correction is either not available or deactivated in all spaceborne GPS receivers.

3.1. Simulated Scenario

[11] To check the validity of the theoretical analysis, an assessment with simulated data has been carried out. For this purpose, a Spirent GSS7790 GPS signal simulator [*Spirent*, 2004; Spirent GSS7790 signal simulator data sheet, available at http://www.positioningtechnology. co.uk/datasheets/gss7790/7790.pdf] has been used to simulate the GPS signal as seen by a receiver onboard a LEO satellite in a Sun-synchronous, polar orbit at 515 km altitude. Ionospheric path delays in the simulator have been modeled using a constant VTEC of 10 TECU and the Lear mapping function. Single-frequency single point navigation solutions computed for different elevation masks have been obtained using a NovAtel OEM4-G2 (NovAtel OEM4-G2 data sheet, available at http:// www.novatel.ca/Documents/Papers/oem4g2l.pdf, and NovAtel OEM4 family user manual, available at http:// www.novatel.ca/Documents/Manuals/om-20000046.pdf) receiver with disabled altitude and speed limitations. Reference position values provided by the signal simulator have been used to obtain the errors in the radial, along-track and cross-track direction.

[12] These errors are summarized in Table 2. As expected, an unbiased estimate of the along-track and cross-track component is achieved, while the radial component exhibits a mean offset that varies with the elevation cutoff angle. The standard deviation of the individual position components reflects the geometric dilution of precision (which is 2−3 times higher in the vertical direction than in horizontal direction) and the pseudorange measurement noise of the employed GPS receiver (which increases for low-elevation satellites because of a less favorable antenna gain). The mean biases in radial direction are found to be in good agreement with the predicted values from Table 1 for a 10 TECU VTEC. A maximum difference of 13% is obtained for a 0° elevation mask, which may be attrib-

uted to the fact that not all visible satellites can be simulated and tracked at very low elevations (<2°).

3.2. Real Scenario

[13] In addition to simulated scenarios, the validity of the derived model has been assessed with real flight data, in which additional error sources such as multipath are present. For this purpose, data from the CHAMP satellite have been used. This satellite carries a BlackJack dual-frequency GPS receiver and orbits the Earth at a nominal altitude of 450 km (CHAMP).

[14] A first and necessary step to assess the effect of the ionospheric delay onto the radial error in a real scenario is to compute the VTEC above the satellite. This has been done using the dual-frequency code and phase data given by the BlackJack receiver. The obtained VTEC values then serve as a reference in the subsequent analysis of the correlation between the radial position error and the VTEC.

3.2.1. VTEC Retrieval

[15] As discussed above, the ionospheric delay that affects the GPS signal is directly proportional to the slant total electron content (STEC). The STEC can readily be obtained using the ionospheric combination

$$P_I = P_2 - P_1$$
$$= \frac{0.105\,\text{m}}{\text{TECU}} \cdot \text{STEC} + \text{DCB}_{\text{GPS}} + \text{DCB}_{\text{Rx}} + \varepsilon \quad (16)$$

of the dual-frequency P(Y) code measurements. Here DCB_{GPS} and DCB_{Rx} are the differential code biases for the GPS satellite and the receiver respectively, while ε comprises the receiver noise and multipath.

[16] Code biases caused by the GPS satellites themselves can be computed using the method described by *Sardón et al.* [1994] and *Sardón and Zarraoa* [1997] but are also available as part of global ionospheric maps (GIM). For this work, DCB_{GPS} values provided with the GIM products of the International GPS Service [*Feltens and Schaer*, 1998] have been adopted. On the other hand, the receiver related code biases (DCB_{Rx}) have been estimated for the employed data arcs using a method proposed by *Heise et al.* [2004]. The method makes use of slant TEC values predicted from a three-dimensional electron density model. For the present study a slightly modified approach was adopted, in which GIM-based VTEC values were scaled to the LEO altitude using a Chapman profile and converted to slant TEC using the Lear mapping function. Using the modeled slant TEC values as well as the known DCBs of the GPS satellites, equation (16) can be solved for the receiver induced differential code bias DCB_{Rx}. The necessary dual-frequency GPS measurements are collected during conditions of low ionospheric activity (high latitude, high elevations and nighttime), for which the error in a
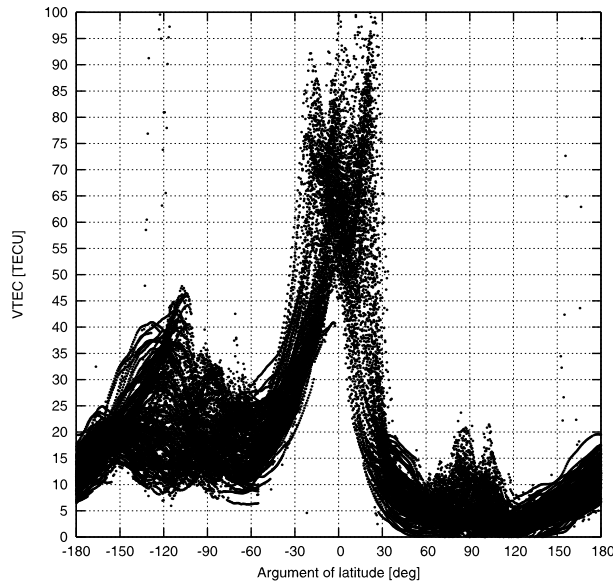
Figure 1. Measured VTEC for the CHAMP satellite on 13 November 2001. The plot shows the variation of the VTEC above the CHAMP satellite against the argument of latitude for all orbits during this day. Arguments of latitude $0°$ and $180°$ correspond to the equator, while $+90°$ and $-90°$ correspond to the extreme northern and southern latitude, respectively.

given ionospheric model is considered to be smallest. The DCBs values for the CHAMP BlackJack receiver obtained in this way vary between 2.4 m and 4.0 m (corresponding to $15-25$ TECU) and are in good overall accord with values independently derived by *Heise et al.* [2004].

[17] Once the ambiguity terms for each data arc and GPS satellite and the differential code biases are accounted for, the STEC is obtained and transformed to VTEC using again the Lear mapping function. As a particular example of VTEC retrieval for the CHAMP satellite is shown in Figure 1. It shows the VTEC for all orbits computed from all visible GPS satellites during this day. The passes through the tails of the Southern and Northern Equatorial Anomalies [see, e.g., *Davies*, 1990], at 18 hours local time, can be seen around $0°$ argument of latitude.

[18] With the above method, each observed GPS satellite at a given epoch provides an independent VTEC measurement. By averaging these measurements, the VTEC above the LEO has been obtained. These measurements correspond to observations at different elevations, however the discrepancy of the real VTEC and the one derived from the STEC using a mapping function

increases with decreasing elevation. Therefore lower elevations should be avoided in performing this analysis. In this work, to minimize the impact of the mismodeling generated in the transformation from STEC to VTEC using a mapping function, only the observations with elevations larger than $40°$ have been considered.

[19] For the subsequent analysis, these values have been averaged to obtain a single VTEC value per epoch. In forming this average, only observations with elevations larger than $40°$ have been considered. In this way the impact of mismodeling caused by the use of an approximate mapping function has been minimized.

3.2.2. Radial Error and VTEC

[20] Despite additional error sources such as noise and multipath, the relationship between the radial error component and the VTEC above the satellite can also be seen in data from real LEO satellites. As a particular example, Figure 2 compares both quantities for the CHAMP satellite on 13 November 2001. Even though the reference values for the vertical TEC have been obtained by use of dual-frequency GPS measurements, the employed single point position solutions are exclusively based on L1 C/A code measurements applying a $10°$ elevation mask. To assess the error of the single frequency kinematic solution, use has been made of precise orbit determination estimates provided by the Jet Propulsion Laboratory, with an inherent accuracy of 10 cm. Using this reference, a mean offset of almost 10 m occurs in the radial direction, while the horizontal position solution is essentially unbiased.

[21] As opposed to the simplified model and the signal simulator test, the radial position error and the instantaneous VTEC are no longer strictly proportional in the real world case. This is due to regional variations of the electron density combined with an irregular distribution of satellites, variations in the dilution of precision, measurement errors, etc. Nevertheless, a high correlation of the radial position error and the instantaneous VTEC is still obvious from Figure 2. To further assess this correlation a scatterplot of both quantities and a comparison with the expected proportionality ratio of 0.52 m/TECU for a $10°$ elevation mask (cf. Table 1) is given in Figure 3. Individual measurements exhibit a scatter of typically $4-5$ m about the theoretical relation.

[22] Besides providing a better understanding of single-frequency GPS navigation errors, the proportionality discussed above might also be used to infer the total electron content above the orbit of a LEO satellite provided that the radial position error can independently be determined. This is indeed possible through a dynamic filtering of the navigation solution using established orbit determination techniques. As discussed by *Gill and Montenbruck* [2004] accuracies of $1-2$ m (3-D RMS) can be achieved in this manner

and the radial position component can be recovered with a typical accuracy of 0.5 m. This, however, is much smaller than the scatter observed in Figure 3 as a result of noise in the single point navigation solution and the employed reference VTEC values. Accounting for the various uncertainties and error sources it appears feasible to derive the instantaneous VTEC from the single point navigation solutions with a standard deviation of about 8–10 TECU.

[23] While this is certainly much worse than what could be achieved with more sophisticated analysis methods (for example use of code carrier divergence or dual-frequency data), the proposed concept does not require access to raw GPS measurements at all. Instead it requires navigation solutions only, which are routinely provided by spaceborne GPS receivers for onboard purposes and ground-based mission operations. As mentioned above, the required reference orbit for retrieving the radial position errors can itself be determined from this data set through dynamical filtering. The method is thus applicable to a wide range of orbiting spacecraft that use a single-frequency GPS receiver for navigation purposes only but have not made and provision for downloading huge sets of raw data for scientific data analysis. The moderate accuracy is thus at least partly
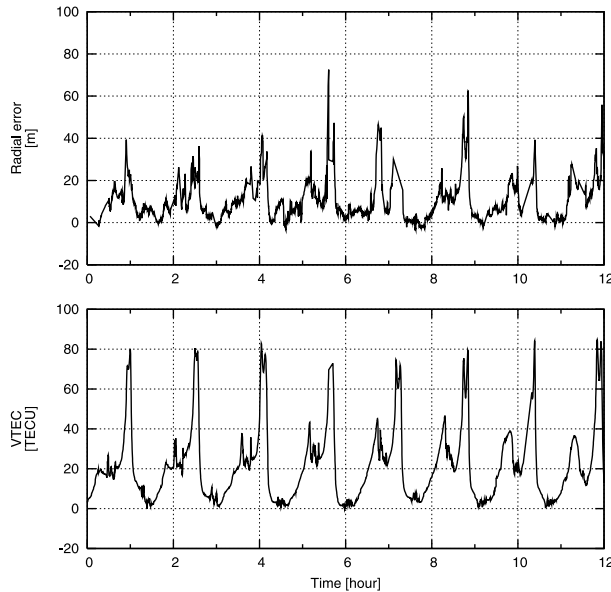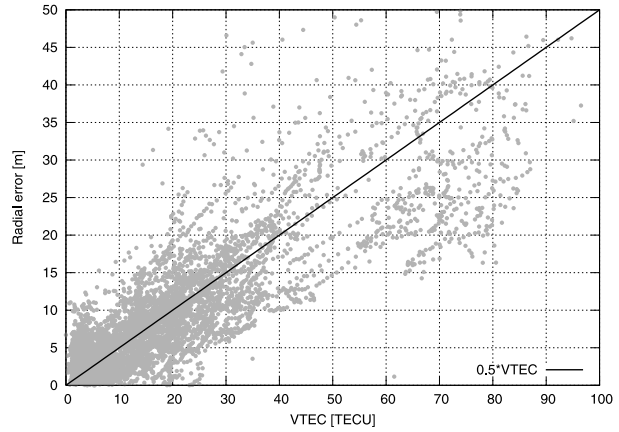

Figure 3. One-to-one comparison of the VTEC above CHAMP and the radial error of the navigation solution on 13 November 2001 for an elevation mask of 10°. The solid line describes the theoretical relation $\Delta r_T = 0.5$ m/TECU × VTEC.

compensated by a wider applicability and better regional and temporal coverage.

4. Summary and Conclusions

[24] A theoretical model for single-frequency GPS navigation errors due to ionospheric path delays has been derived for spacecraft in low Earth orbit. The result of this analysis evidences a linear relationship between the ionospheric VTEC and the radial position error as well as the clock offset error of the single point navigation solution. On the contrary, it is shown that the horizontal position components are essentially unaffected by the ionospheric delay. Moreover, it has been shown that the radial position error depends as well on the elevation mask and decrease by roughly one third when constraining the observations to elevations above 10°. as compared to a full hemispherical coverage. The relation between the VTEC and the position error that has been derived in this paper holds for receivers that ignore the ionospheric effect to obtain the single-frequency navigation solution, which is the case for the majority of spaceborne GPS manufacturers. To correctly interpret the biases in the radial error it is required a knowledge on the elevation mask set in the receiver. The theoretical analysis has been also substantiated with actual GPS measurements collected in a signal simulator test bed as well as data from the CHAMP satellite.

[25] Besides being of interest for the assessment of LEO satellite navigation accuracies, the established relationship might also be of interest for the derivation of coarse TEC values above the spacecraft orbit from single point navigation solutions. While limited in accuracy it

Figure 2. Comparison of (top) the radial position error and (bottom) the VTEC above the CHAMP satellite for 13 November 2001. Single-frequency navigation solutions have been computed with a 10° elevation mask. VTEC values are derived from dual-frequency GPS data as explained in the text.

offers a great simplicity and can be applied to a wide range of orbiting spacecraft.

References

Berthias, J. A., P. Broca, A. Comps, S. Gratton, D. Laurichesse, and F. Mercier (2001), Lessons learned from the use of a GPS receiver in less than optimal conditions, paper presented at 16th International Symposium on Space Flight Dynamics, Jet Propul. Lab., Pasadena, Calif., 3–6 Dec.

Davies, K. (1990), *Ionospheric Radio*, *IEE Electromagn. Waves Ser.*, vol. 31, Peter Peregrinus, London.

Feltens, J., and S. Schaer (1998), IGS products for the ionosphere, paper presented at IGS Analysis Center Workshop, Eur. Space Oper. Cent., Eur. Space Agency, Darmstadt, Germany.

Gill, E., and O. Montenbruck (2004), Comparison of GPS-based orbit determination strategies, paper presented at 18th International Symposium on Space Flight Dynamics, Ger. Aerosp. Cent., Munich, Germany, 11–14 Oct.

Heise, S., C. Stolle, S. Schlter, and N. Jakowski (2004), Differential code bias of GPS receivers in low Earth orbit: An assessment for CHAMP and SAC-C, in *CHAMP Mission Results for Gravity and Magnetic Field Mapping, and GPS Atmosphere Sounding*, edited by C. Reigber et al., pp. 465–470, Springer, New York.

Hwang, Y., and G. H. Born (2005), Orbit determination strategy using single-frequency global-positioning-system data, *J. Spacecr. Rockets*, 42(5), 896–901.

Klobuchar, J. A. (1996), Global Positioning System: Theory and applications, in *Ionospheric Effects in GPS*, vol. 1, edited by B. W. Parkinson and J. J. Spilker, chap. 12, pp. 485–515, AIAA Publ., Washington, D. C.

Lear, W. M. (1987), GPS navigation for low-Earth orbiting vehicles, *NASA 87-FM-2, JSC-32031*, rev. 1, Lyndon B. Johnson Space Cent., Houston, Tex.

Misra, P., and P. Enge (2001), *Global Positioning System: Signals, Measurements, and Performance*, Ganga-Jamuna Press, Lincoln, Mass.

Montenbruck, O. (2003), Kinematic GPS positioning of LEO satellites using ionosphere-free single frequency measurements, *Aerosp. Sci. Technol.*, 7, 396–405.

Montenbruck, O., and E. Gill (2002), Ionospheric correction for GPS tracking of LEO satellites, *J. Navig.*, 55, 293–304.

Montenbruck, O., and M. Markgraf (2003), Ionospheric electron density profiles from single frequency GPS tracking of sounding rockets, *Tech. Note TN03-07*, Ger. Space Oper. Cent., Dtsch. Zent. für Luft- und Raumfahrt, Munich, Germany.

Sardón, E., and N. Zarraoa (1997), Estimation of total electron content using GPS data: How stable are the differential satellite and receiver instrumental biases?, *Radio Sci.*, 32(5), 1899–1910.

Sardón, E., A. Rius, and N. Zarraoa (1994), Estimation of the transmitter and receiver differential biases and the ionospheric total electron content from Global Positioning System observations, *Radio Sci.*, 29(3), 577–586.

Spirent (2004), SimGEN (including SimLocate) user manual: Software for the Spirent range of satellite navigation simulator products, issue 1-13, *Doc. DGP 00686AAA*, Crawley, U. K.

Van Dierendonck, A. J., J. Klobuchar, and Q. Hua (1993), Ionospheric scintillation monitoring using commercial single frequency C/A code receivers, paper presented at ION GPS-93 Conference, Inst. of Navig., Salt Lake City, Utah.

Yoon, J.-C., K.-M. Roh, E.-S. Park, B.-Y. Moon, K.-H. Choi, J.-S. Lee, B.-S. Lee, J. Kim, and Y.-K. Chang (2002), Orbit determination of spacecraft using Global Positioning System single frequency measurements, *J. Spacecr. Rockets*, 39(5), 796–801.

Yunck, T. P. (1996), Orbit determination, in *Global Positioning System: Theory and Applications*, vol. 1, edited by B. W. Parkinson and J. J. Spilker, chap. 21, pp. 559–592, AIAA Publ., Washington, D. C.

Yunck, T. P., W. I. Bertiger, S. C. Wu, Y. Bar-Sever, E. J. Christiensen, B. Haines, S. M. Lichten, R. J. Muellerschoen, Y. Vigue, and P. Willis (1994), First assessment of GPS-based reduced dynamic orbit determination on TOPEX/Poseidon, *Geophys. Res. Lett.*, 21, 541–544.

M. Garcia-Fernàndez and O. Montenbruck, German Space Operation Center, Deutsches Zentrum fur Luft- und Raumfahrt, D-82234Wessling, Germany. (miquel.garcia@dlr.de)